

# Alkoxy(tetraaryl)silicates bearing 9,10-disilatriptycene skeleton

Shintaro Ishida  | Minori Takiguchi | Takeaki Iwamoto 

Department of Chemistry, Graduate School of Science, Tohoku University, Sendai, Japan

## Correspondence

Shintaro Ishida and Takeaki Iwamoto, Department of Chemistry, Graduate School of Science, Tohoku University, Sendai, Japan.

Emails: ishida@tohoku.ac.jp; takeaki.iwamoto.b8@tohoku.ac.jp

## Abstract

As anionic five-coordinate silicon species (five-coordinate silicates) exhibit high reactivity and unique fluxional behavior, their structure and property have received substantial attention. We report herein synthesis, structure, and fluxional behavior of alkoxy(tetraaryl)silicates having the 9,10-disilatriptycene skeleton (**6<sup>-</sup>** and **7<sup>-</sup>**). The molecular structure of the cryptate salt [Li(crypt-222)]<sup>+</sup>**7<sup>-</sup>** shows that the five-coordinate silicon adopts a distorted trigonal bipyramidal structure with oxygen atom occupying an equatorial position. In the <sup>1</sup>H and <sup>13</sup>C{<sup>1</sup>H} NMR spectra of [Li(crypt-222)]<sup>+</sup>**7<sup>-</sup>**, a set of signals due to *o*-phenylene blades in **7<sup>-</sup>** was observed at room temperature, which indicates fluxional behavior of **7<sup>-</sup>** on the NMR timescale. Computational study suggests that the observed process proceeds via a 120° rotation of bidentate ligand around the Si-Si axis that consists of two sequential Berry pseudorotations.

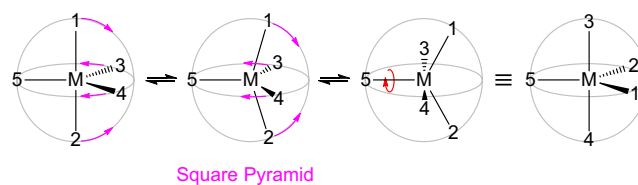
## 1 | INTRODUCTION

Four-coordinate silicon can accept a nucleophile to form five-coordinate silicon species (five-coordinate silicates).<sup>[1]</sup> Because silicates are regarded as key intermediates for numerous reactions such as Tamao oxidation,<sup>[2]</sup> Hiyama coupling,<sup>[3]</sup> silyl migrations,<sup>[4]</sup> and dehydrogenative silylation,<sup>[5]</sup> their structure and property have attracted considerable attention even in recent years. In general, five-coordinate silicates prefer trigonal bipyramidal geometries and exhibit a facile fluxional behavior due to the intramolecular stereomutation with a small activation barrier. This process is interpreted as a Berry pseudorotation (BPR) that proceeds via a square pyramidal structure during molecular motion as shown in Scheme 1.<sup>[1,6]</sup> Although turnstile rotation (TR) between three ligands (*trio*) and two ligands (*duo*) was proposed as another possible mechanism to explain the fluxional behavior,<sup>[7]</sup> Couzijn and Lammertsma<sup>[8]</sup> have revealed that TR is equivalent to BPR by a topological analysis.

Several studies on the dynamic behavior of well-designed anionic five-coordinate silicates **A-H** having two bidentate

ligands (Figure 1)<sup>[9]</sup> indicate that stereomutations of anionic five-coordinate silicates are greatly influenced by the bidentate ligands. In group-15 element chemistry, five-coordinate antimony compounds **I** and **J** having rigid tridentate ligand exhibit fluxional behavior due to the TR induced by the geometrical constraint.<sup>[10,11]</sup> Therefore, anionic five-coordinate silicates bearing tridentate ligands should give further information on their fluxionality and the mechanisms of stereomutation.

Previously, we reported a facile synthesis of 9-phenyl-9,10-disilatriptycene (**1**) by the reaction of bis(2-bromophenyl)silane (**2**) with magnesium under a microwave heating condition (Scheme 2).<sup>[12]</sup> As Grignard reagent **3** formed as an intermediate in this reaction, a functional group can be introduced on the 2-position of the external phenyl ring. Thus, we planned to synthesize alkoxy(tetraaryl)silicates having 9,10-disilatriptycene skeleton (Figure 2) that



**SCHEME 1** Berry pseudorotation of five-coordinate species

Dedicated to 82nd birthday of Professor Naomichi Furukawa.

Contract grant sponsor: JSPS KAKENHI

Contract grant number: JP25708004

Contract grant number: JP25620020

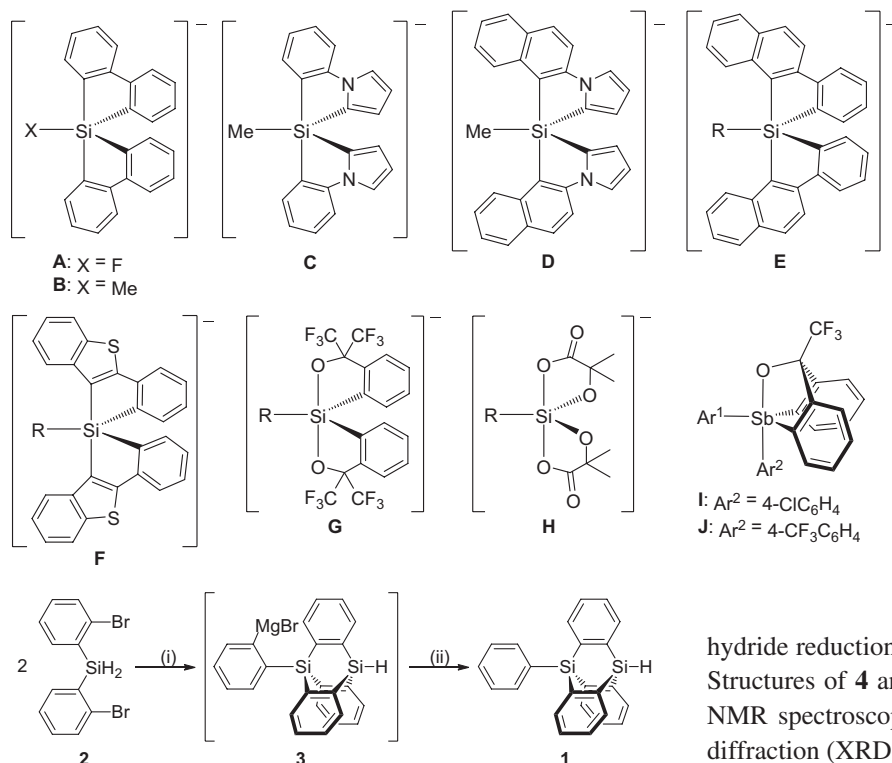


**FIGURE 1** Structurally constrained anionic five-coordinate silicates **A–H** and neutral five-coordinate stiboranes **I** and **J** having a tridentate ligand (Ar<sup>1</sup> = 3,5-Me<sub>2</sub>C<sub>6</sub>H<sub>3</sub>)

hydride reduction of **4** with LiAlH<sub>4</sub> afforded **5** in 83% yield. Structures of **4** and **5** were determined by a combination of NMR spectroscopy, MS spectrometry, single crystal X-ray diffraction (XRD) study, and elemental analysis.

**SCHEME 2** Synthesis of **1** via **3**. (i) Mg, THF, reflux or microwave heating (150°C); (ii) aqueous work-up

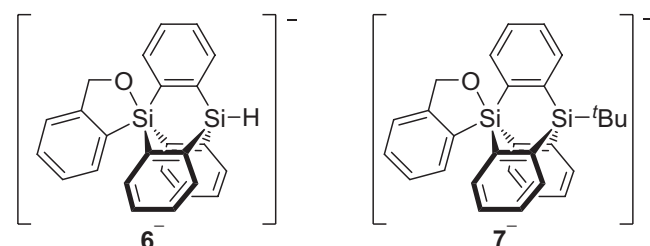


**FIGURE 2** Alkoxy(tetraaryl)silicates **6<sup>-</sup>** and **7<sup>-</sup>**

would give information on the dynamics behavior derived by the combination of the rigid tridentate and bidentate ligands on the five-coordinate silicon. We report herein (a) synthesis of new alkoxy(tetraaryl)silicates **6<sup>-</sup>** and **7<sup>-</sup>** having 9,10-disilatriptycene skeleton, (b) molecular structure of [Li(crypt-222)]<sup>+</sup>**7<sup>-</sup>** (crypt-222 = [2.2.2]cryptand), and (c) dynamic behavior of **7<sup>-</sup>** in solution. In addition, fundamental properties of the newly synthesized 9,10-disilatriptycene derivatives are also presented.

## 2 | RESULTS AND DISCUSSION

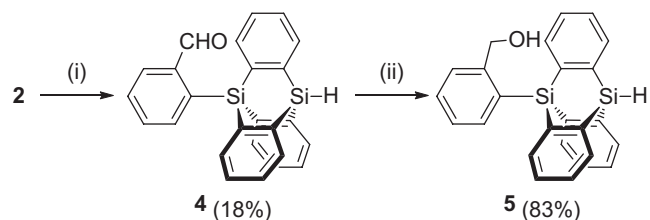
### 2.1 | Synthesis

As shown in Scheme 3, 2-formylphenyl derivative **4** was prepared by the reaction of in situ generated **3** from **2**<sup>[13]</sup> with DMF in 18% isolated yield (based on **2**). The subsequent

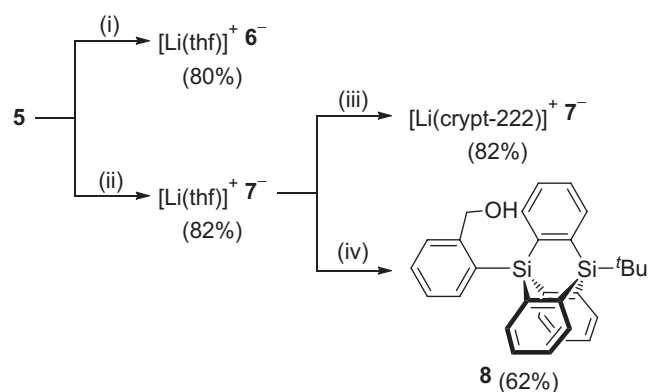
Treatment of **5** with an equimolar amount of *tert*-butyllithium in THF at −78°C afforded desired five-coordinate silicate salt [Li(thf)]<sup>+</sup>**6<sup>-</sup>** in 80% yield (Scheme 4). A similar reaction of **5** with two equivalent of *tert*-butyllithium gave *tert*-butylated silicate [Li(thf)]<sup>+</sup>**7<sup>-</sup>** in 82%. In this reaction, the second *tert*-butyllithium reacted as a nucleophile toward the Si–H moiety of **6<sup>-</sup>**. Hydrolysis of [Li(thf)]<sup>+</sup>**7<sup>-</sup>** gave benzylalcohol derivative **8** in 62% yield. Exchange of the ligand on the lithium cation from THF to [2.2.2]cryptand (abbreviated as crypt-222) increased the stability and crystallinity of the silicate, and [Li(crypt-222)]<sup>+</sup>**7<sup>-</sup>** salt was successfully isolated and spectroscopically and structurally characterized.

### 2.2 | Molecular structures of neutral 9,10-disilatriptycenes

Solid state structures of neutral 9,10-disilatriptycene derivatives (**4**, **5**, **8**) are shown in Figures 3–5. In compounds **4**, **5** and **8**, the closest distances between oxygen and silicon atoms (intramolecular O1 and Si1 distances) are 4.38, 4.26, and 4.26 Å, respectively. These distances are much longer than the sum of the van der Waals radii ( $\Sigma r_{vdW}$ ) of silicon and oxygen atoms (3.62 Å).<sup>[14]</sup> Thus, no significant bonding interaction exists between these atoms. Hydrogen bonding of hydroxy groups was not found in the crystal of **5**; the shortest intermolecular distance between oxygen atoms was 7.54 Å, while dimeric structure by hydrogen bonding was observed in the packing diagram of **8** (intermolecular O...O distance of 2.63 Å, Figure S2). The averaged bond lengths of Si1–C(*o*-phenylene) and



**SCHEME 3** Synthesis of **4** and **5**. (i) THF reflux with Mg, followed by excess DMF at 0°C for 1 h; (ii) ether with LiAlH<sub>4</sub> (0.5 eq.) at 0°C for 40 min



**SCHEME 4** Synthesis of silicates **6<sup>-</sup>** and **7<sup>-</sup>** and benzyl alcohol **8**. (i) *tert*-Butyllithium (1.0 eq.) in THF, -78°C for 1 h; (ii) *tert*-butyllithium (2.3 eq.) in THF, -78°C for 1 h; (iii) crypt-222 (1.0 eq.) in toluene at room temperature for 1 day. (iv) Aqueous work-up

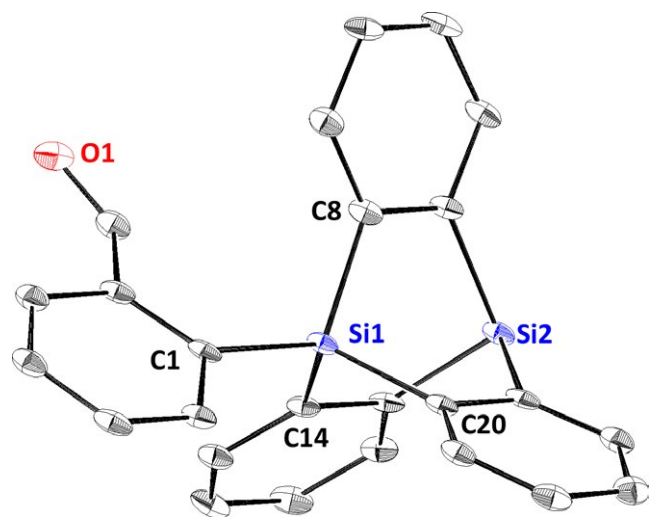


**FIGURE 3** Molecular structure of **4**. Hydrogen atoms are omitted for clarity. Thermal ellipsoids are drawn at the 50% probability level. Selected bond lengths (Å) and angles (°); Si1–C1 1.881(2), Si1–C8 1.890(2), Si1–C14 1.894(2), Si1–C20 1.895(2), C1–Si1–C8 115.40(9), C1–Si1–C14 110.92(9), C8–Si1–C14 103.71(9), C1–Si1–C20 118.52(9), C8–Si1–C20 103.02(9), C14–Si1–C20 103.62(9)

Si1–C(2-substituted phenyl) [1.891(3) and 1.880(3) Å] are slightly elongated from the standard Si–C bond length of 1.86 Å.

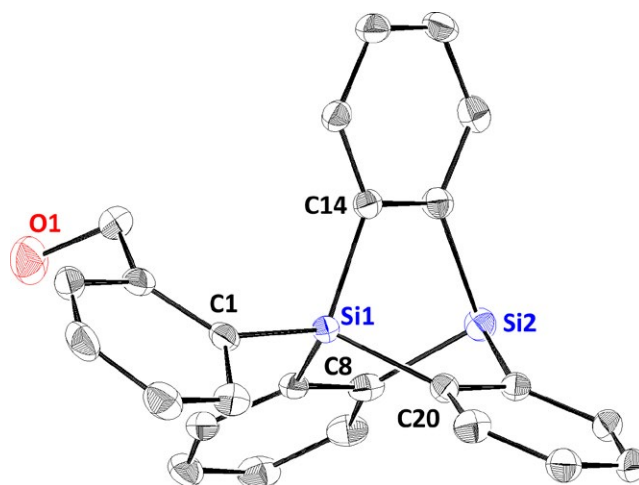


**FIGURE 4** Molecular structure of **5**. Hydrogen atoms are omitted for clarity. Thermal ellipsoids are drawn at the 50% probability level. Selected bond lengths (Å) and angles (°); Si1–C1 1.877(4), Si1–C8 1.890(4), Si1–C14 1.898(4), Si1–C20 1.899(4), C1–Si1–C8 112.45(17), C1–Si1–C14 117.08(18), C8–Si1–C14 102.45(17), C1–Si1–C20 116.79(18), C8–Si1–C20 104.96(17), C14–Si1–C20 101.31(17)

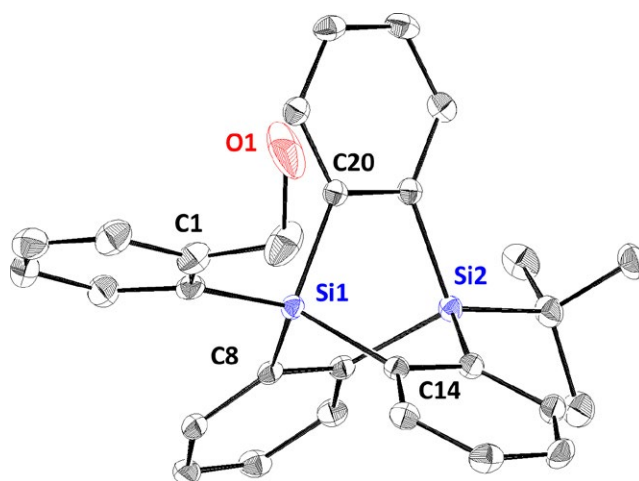


**FIGURE 5** Molecular structure of **8**. Hydrogen atoms are omitted for clarity. Thermal ellipsoids are drawn at the 50% probability level. A disorder was found in the OH moiety with the occupancy factors of 0.51 and 0.49, and a hydroxy group is shown. Selected bond lengths (Å) and angles (°); Si1–C1 1.8828(17), Si1–C8 1.8797(17), Si1–C14 1.8885(16), Si1–C20 1.8806(17), C1–Si1–C8 115.63(8), C1–Si1–C14 121.32(7), C1–Si1–C20 107.96(7), C8–Si1–C14 100.66(7), C8–Si1–C20 105.08(7), C14–Si1–C20 104.64(7)

### 2.3 | Molecular structure of silicate

Molecular structure of [Li(crypt-222)]<sup>+</sup>7<sup>-</sup> obtained by XRD analysis revealed that the salt is a solvent separated ion pair; the cationic part [Li(crypt-222)]<sup>+</sup> is well-separated from the counter anion (Figure S1). In anion part, oxygen atom (O1) coordinates to silicon (Si1) to form a five-coordinate silicate as shown in Figure 6; the Si1–O1 length of 1.7428(14) Å is

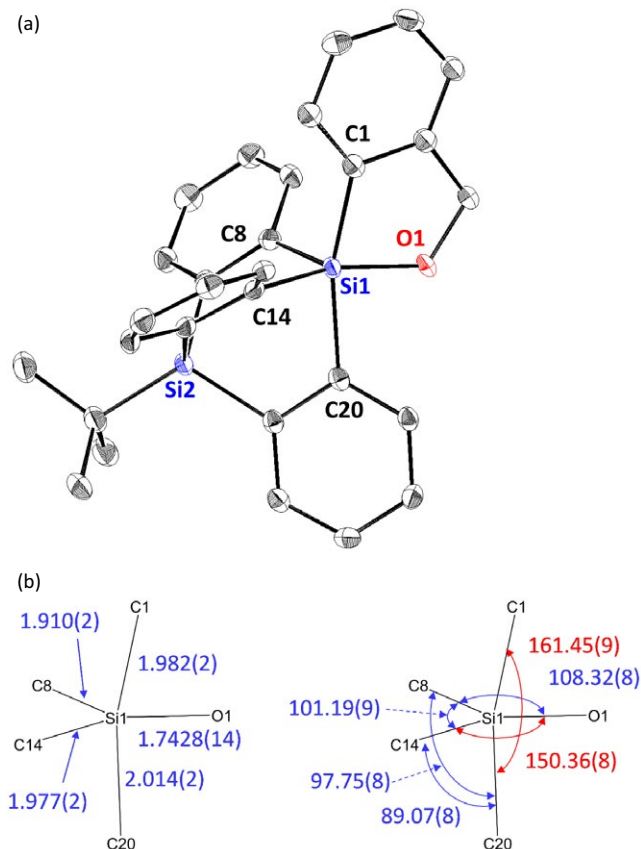


**FIGURE 6** A, Molecular structure of  $[\text{Li}(\text{crypt-222})]^+7^-$ . Counter cation  $[\text{Li}(\text{crypt-222})]^+$  and hydrogen atoms are omitted for clarity. Thermal ellipsoids are drawn at the 50% probability level. B, Bond lengths (Å) and angles ( $^\circ$ ) around five-coordinate silicon (Si1)

longer than standard tetracoordinate Si–O bonds (1.64 Å) and much shorter than the  $\Sigma r_{\text{vdW}}$  of Si and O atoms (3.62 Å).<sup>[14]</sup> A large bond angle of C1–Si1–C20 [161.45(9) $^\circ$ ] indicates that C1 and C20 atoms occupied the apical positions. To evaluate five-coordinate geometry of  $7^-$ , the indicators of the trigonal bipyramid geometry (%TBP<sub>a</sub> and %TBP<sub>e</sub>)<sup>[15,16]</sup> were used. The %TBP<sub>a</sub> values for C1 and C20 are 87.0 for C1 and 97.9 for C20, and %TBP<sub>e</sub> of 99.6 indicate that five-coordinate silicon of  $7^-$  adopts a distorted trigonal bipyramidal geometry. As the bidentate ligand is positioned on space between two *o*-phenylene blades (C8 and C14) of 9,10-disilatriptycene skeleton to avoid steric congestion, the electronegative O1 atom of the bidentate ligand occupied an equatorial position against the Muetterties rule.<sup>[1,17]</sup> The Si–C bond lengths of five-coordinate silicon are elongated compared to those of tetracoordinate compounds (**4**, **5**, and **8**); the apical Si–C bonds (Si1–C20 and Si1–C1) of 2.014(2) and 1.982(2) Å are longer than those of the equatorial Si–C bonds [Si1–C8 and Si1–C14 1.910(2) and 1.977(2) Å] in  $7^-$ . As shown in Figure 6B, a remarkable large bond angle of O1–Si1–C14 [150.36(8) $^\circ$ ] from that of O1–Si1–C8 [108.32(8) $^\circ$ ] indicates that TBP structure of  $7^-$  deforms somewhat to a square pyramidal (SP) structure

having one axial ligand of C8 and four basal ligands (O1, C1, C14, C20). Shorter bond length of Si1–C8 compared to the other Si1–C bonds and a relatively long Si1–O1 bond support that the SP character of  $7^-$  despite the large %TBP values. The observed deformation to the SP structure may arise from the packing forces in the single crystal because several intermolecular contacts between the bidentate ligand of  $7^-$  and neighboring molecules were observed. To the best of our knowledge,  $[\text{Li}(\text{crypt-222})]^+7^-$  is the first isolable alkoxy(tetraaryl)silicate.

## 2.4 | UV-vis absorption and fluorescence spectra

Since UV-vis absorption and emission of several arylsilanes are dependent on the number of the coordination of nucleophiles to form anionic silicates,<sup>[18]</sup> we investigated absorption and emission of compounds **4–8**. Absorption and fluorescence maxima of 9,10-disilatriptycenes **4**, **5**, **8**, and  $[\text{Li}(\text{crypt-222})]^+7^-$  are summarized in Table 1, and their spectra are shown in Figures S3–S6 in the Supporting Information. UV-vis absorption spectra of neutral compounds **4**, **5**, and **8** exhibited intense bands around 215 nm and weak bands (<sup>1</sup>L<sub>b</sub> band) around 275 nm. The position of <sup>1</sup>L<sub>b</sub> band of anionic silicate  $[\text{Li}(\text{crypt-222})]^+7^-$  (276 nm) is not significantly shifted compared to those of the neutral species. In compound **4**, an additional very weak absorption band due to *n*→ $\pi^*$  transition appeared around 343 nm. In the fluorescence spectra, a broad emission band of  $[\text{Li}(\text{crypt-222})]^+7^-$  appeared around 350 nm, and the position of the band was similar to those of **5** and **8**. Consequently, coordination of alkoxide to the silicon atom of 9,10-disilatriptycene skeleton to form anionic silicate does not remarkably affect the absorption and fluorescence spectra. Compound **4** was nonfluorescent as well as common aryl carbonyl compounds.<sup>[19]</sup>

## 2.5 | Molecular structures in solution

<sup>29</sup>Si NMR chemical shifts of 9,10-disilatriptycenes (**4–8**) are summarized in Table 2. The <sup>29</sup>Si NMR signals of

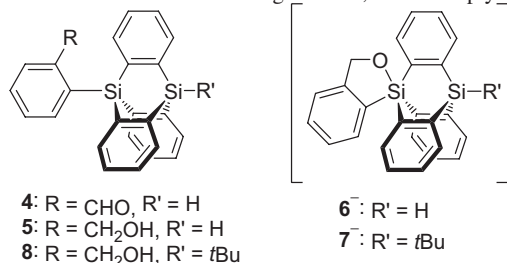
**TABLE 1** Photophysical parameters of **4**, **5**,  $[\text{Li}(\text{crypt-222})]^+7^-$ , and **8**

Compound	$\lambda_{\text{max}}/\text{nm}$ ( $\epsilon/\text{mol}^{-1} \text{dm}^3 \text{cm}^{-1}$ )	$\lambda_{\text{em}}/\text{nm}$
<b>4</b> <sup>a</sup>	213 ( $1.0 \times 10^5$ ), 281 ( $3.0 \times 10^3$ ), 343 ( $7.0 \times 10$ )	Not detected
<b>5</b> <sup>a</sup>	215 ( $8.1 \times 10^4$ ), 274 ( $1.9 \times 10^3$ )	356
<b>8</b> <sup>a</sup>	215 ( $8.0 \times 10^4$ ), 274 ( $1.7 \times 10^3$ )	353
$[\text{Li}(\text{crypt-222})]^+7^-$ <sup>b</sup>	276 ( $2.8 \times 10^3$ )	349

<sup>a</sup>In hexane.

<sup>b</sup>In THF.

<sup>c</sup>Excited at 250 nm.

**TABLE 2**  $^{29}\text{Si}$  NMR signals of 9,10-disilatriptycenes

Compound	Solvent	Chemical shift/ppm
4	Chloroform- <i>d</i>	-39.0, -36.6
5	Chloroform- <i>d</i>	-39.2, -36.6
8	Chloroform- <i>d</i>	-40.0, -32.3
[Li(thf)] <sup>+</sup> 6 <sup>-</sup>	DMSO- <i>d</i> <sub>6</sub>	-104.4, -41.1
[Li(thf)] <sup>+</sup> 7 <sup>-</sup>	DMSO- <i>d</i> <sub>6</sub>	-105.2, -37.5
[Li(crypt-222)] <sup>+</sup> 7 <sup>-</sup>	DMSO- <i>d</i> <sub>6</sub>	-105.2, -37.5

tetracoordinate silicon atoms in the compounds resonate in the range of -36.6 to -41.1 ppm. The signals observed at -104.4 for 6<sup>-</sup> and -105.2 ppm for 7<sup>-</sup> in DMSO-*d*<sub>6</sub> can be assigned to the five-coordinate silicon nuclei because typical five-coordinate silicon nuclei exhibit signals at these regions.<sup>[1,20]</sup> These results are consistent with the five-coordinate silicate structures of 6<sup>-</sup> and 7<sup>-</sup> in DMSO-*d*<sub>6</sub>.

Noticeably, the obtained silicates exhibited fluxional behavior. As shown in Figure 7,  $^{13}\text{C}\{^1\text{H}\}$  NMR spectrum of [Li(crypt-222)]<sup>+</sup>7<sup>-</sup> in DMSO-*d*<sub>6</sub> showed six signals due to the three blades of the 9,10-disilatriptycene moiety at 300 K, which indicates that two equatorial and one apical blades of 9,10-disilatriptycene exchange their positions on the NMR timescale. Similar  $^{13}\text{C}\{^1\text{H}\}$  NMR signal patterns of [Li(thf)]<sup>+</sup>6<sup>-</sup> and [Li(thf)]<sup>+</sup>7<sup>-</sup> were obtained in DMSO-*d*<sub>6</sub>. Then, we focused

on the temperature dependence of the fluxional behavior of [Li(crypt-222)]<sup>+</sup>7<sup>-</sup> in THF-*d*<sub>8</sub>. In the  $^1\text{H}$  NMR spectra of [Li(crypt-222)]<sup>+</sup>7<sup>-</sup> at various temperatures, signals of blades split into two sets of signals with 2:1 integral ratio in lower temperatures (Figure 8). The rate constants of the dynamic process at each temperature can be determined by line-shape analysis using well-separated signals of 8.37 and 7.06 ppm at 193 K, and the kinetic parameters for the dynamic behavior derived from an Eyring plot (Table S5) were as follows:  $\Delta H^\ddagger = 40.5 \pm 0.9$  kJ/mol and  $\Delta S^\ddagger = -8.8 \pm 4.1$  J mol<sup>-1</sup> K<sup>-1</sup>. The small  $\Delta S^\ddagger$  value is consistent with an intramolecular process.

## 2.6 | Computational study on the fluxional behavior

In order to get insights into the observed fluxional behavior of [Li(crypt-222)]<sup>+</sup>7<sup>-</sup>, the computational study of 6<sup>-</sup> was carried out at the B3PW91 + D3/6-31 + G(d) level of theory. A transition state (6<sub>TS</sub><sup>-</sup>) that connects two rotamers of 6<sup>-</sup> (6<sub>a</sub><sup>-</sup> and 6<sub>b</sub><sup>-</sup>) was found, which was confirmed by the IRC analysis (vide infra). This process represents a 120° rotation of the bidentate ligand around the Si-Si axis as shown in an animated GIF file (IRC\_trace.gif, Supporting Information) and illustrated in Figure 9. We also calculated an alkoxide (6<sub>t</sub><sup>-</sup>) that has tetracoordinate silicon and can be generated by the heterolytic cleavage of the Si-O bond. The intervention of 6<sub>t</sub><sup>-</sup> in the fluxional behavior would be unlikely because 6<sub>t</sub><sup>-</sup> is much higher in energy by 251.7 kJ/mol from 6<sub>a</sub><sup>-</sup> and by 197.2 kJ/mol from transition state 6<sub>TS</sub><sup>-</sup>. The calculated activation barrier from 6<sub>a</sub><sup>-</sup> to 6<sub>b</sub><sup>-</sup> via 6<sub>t</sub><sup>-</sup> ( $\Delta G^\ddagger = 54.5$  kJ/mol) at 298.15 K is in accord with the experimentally obtained value ( $\Delta G^\ddagger = 43.1 \pm 2.1$  kJ/mol) at the same temperature.

Couzijn and Lammertsma<sup>[8]</sup> have proposed that dynamics of trigonal bipyramidal five-coordinate compounds can

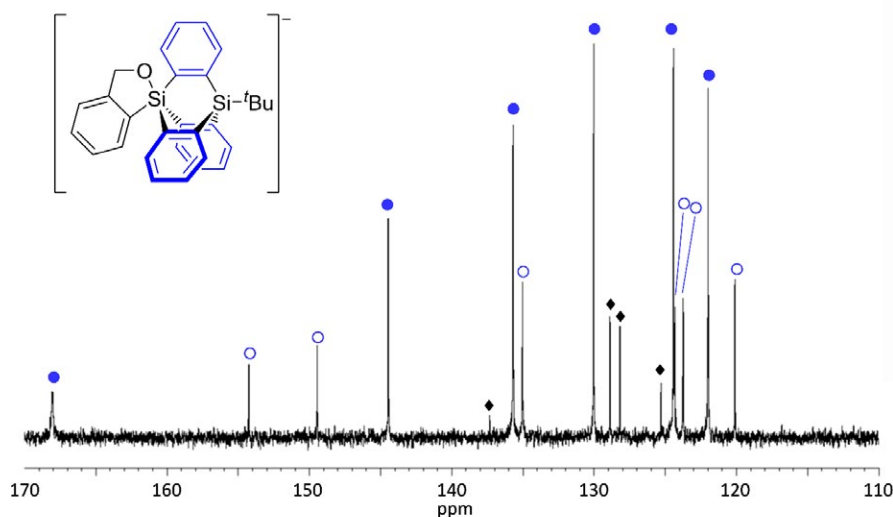


**FIGURE 7** Aromatic region  $^{13}\text{C}\{^1\text{H}\}$  NMR spectrum of [Li(crypt-222)]<sup>+</sup>7<sup>-</sup> in DMSO-*d*<sub>6</sub> at 300 K (♦ = signals of residual toluene). Blue solid and open circles denote the signals of the 9,10-disilatriptycene and alkoxyphenyl moieties, respectively

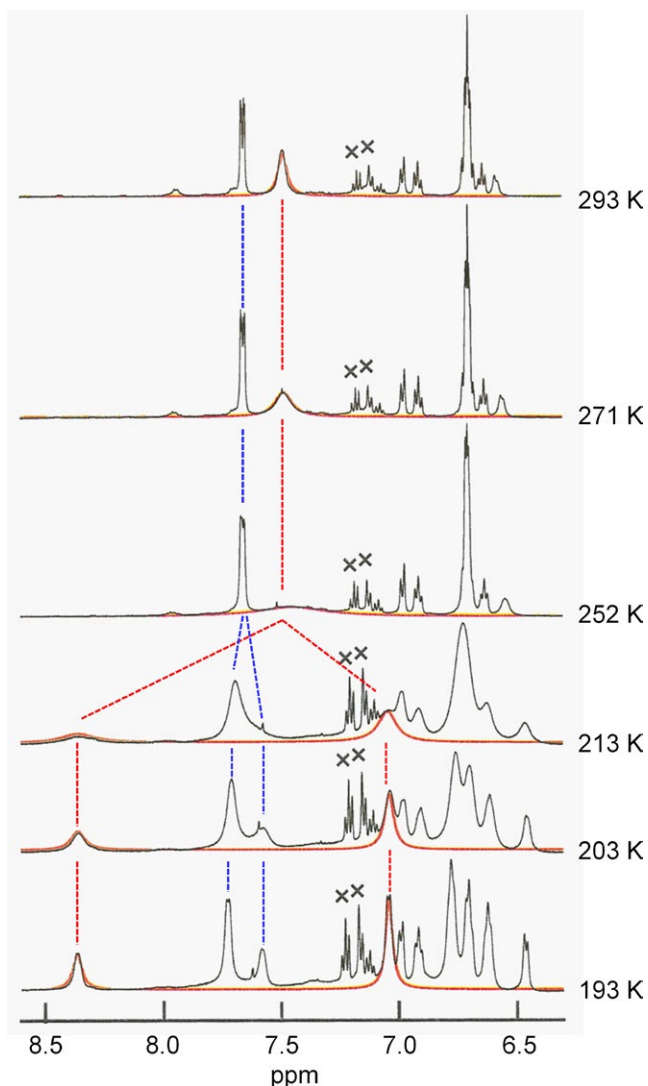


**FIGURE 8**  $^1\text{H}$  NMR spectra of  $[\text{Li}(\text{crypt-222})]^+ 7^-$  at various temperatures (black) and their line-shape simulations (red) using the following parameters:  $\delta_A = 8.373$  ppm,  $\Delta\nu_{1/2} = 17.5$  Hz,  $\delta_B = 7.0556$  ppm,  $\Delta\nu_{1/2} = 15.0$  Hz

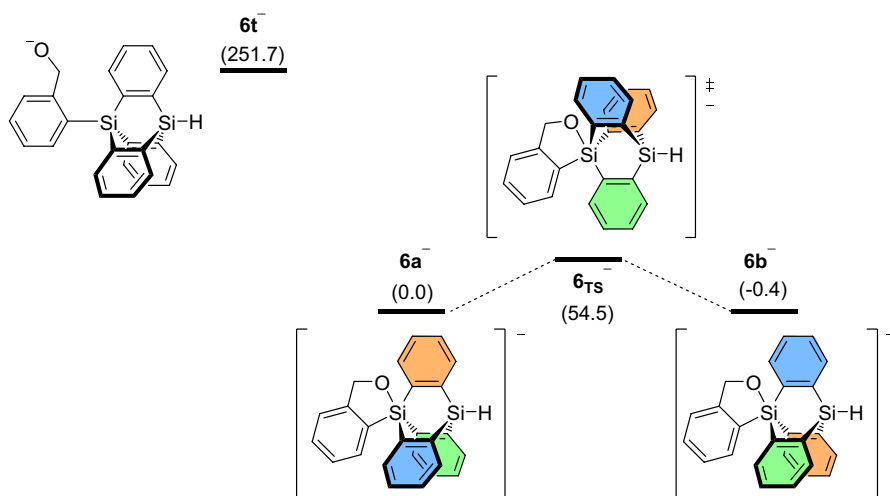


**FIGURE 9** Schematic representation of isomerization path of  $6a^-$  and  $6b^-$  via  $6_{\text{TS}}^-$  with  $6t^-$  predicted at the B3PW91-D3/6-31 + G(d) level of theory. The values in parentheses are the free energies or the activation free energy relative to  $6a^-$  at 298.15 K in  $\text{kJ mol}^{-1}$

be interpreted as a single BPR or a combination of BPRs and each BPR connects two trigonal bipyramidal structures via a square pyramidal structure as a transition state or a nonstationary structure. They introduced the topology parameter (TP) for validating the mechanism of the stereomutation of the five-coordinate species and discussed the change in TP respect to the reaction coordinate by IRC calculation.<sup>[21]</sup> The obtained double V-shaped profile of TP (Figure 10) suggests that the  $120^\circ$  rotation of the bidentate ligand in  $6^-$  consists of two sequential BPRs through two square pyramidal structures. The transition state  $6_{\text{TS}}^-$  adopts distorted trigonal bipyramidal geometry with oxygen atom occupied at the apical position. The obtained topological profile of the stereomutation of  $6^-$  with tridentate and bidentate ligands is similar to those of silicates with two bidentate ligands.<sup>[8]</sup>

### 3 | CONCLUSION

Anionic alkoxy(tetraaryl)silicates  $6^-$  and  $7^-$  having 9,10-disilatriptycene skeleton were synthesized by the reactions of **5** with *tert*-butyllithium, and  $[\text{Li}(\text{crypt-222})]^+ 7^-$  salt was successfully isolated and characterized. In the solid state structure of  $[\text{Li}(\text{crypt-222})]^+ 7^-$ , the five-coordinate silicon adopts distorted trigonal bipyramidal geometry, and a coordinating oxygen atom is located at the equatorial position. On the basis of the  $^{29}\text{Si}$  NMR spectra, compounds  $6^-$  and  $7^-$  exist as five-coordinate silicate structures in  $\text{DMSO-}d_6$  at room temperature. Temperature dependence of the NMR spectra demonstrated that three *o*-phenylene blades of  $7^-$  are chemically equivalent at 300 K, which indicate dynamic behavior of the five-coordinate silicon because two blades are located at the equatorial position and one blade lies at the apical position in the solid structure. The experimentally obtained kinetic parameters of the interchange process are matched with the value estimated

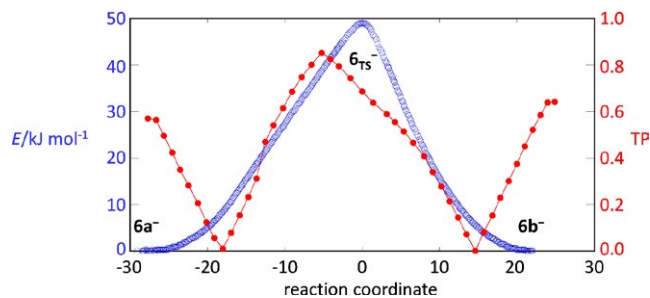


**FIGURE 10** IRC trace with TP of the isomerization of  $6a^-$  to  $6b^-$  via  $6_{TS}^-$ . Blue line = IRC trace, red line = TP value

theoretically. Computational study suggested that the observed stereomutation proceeds via a  $120^\circ$  rotation of the bidentate ligand around the Si-Si axis that consists of two sequential BPRs.

## 4 | EXPERIMENTAL

### 4.1 | General procedures

All synthetic experiments were performed under argon or nitrogen in a standard vacuum system unless otherwise noted.  $^1\text{H}$  (400 MHz),  $^{13}\text{C}\{^1\text{H}\}$  (100 MHz), and  $^{29}\text{Si}\{^1\text{H}\}$  (79 MHz) NMR spectra of products were recorded on a Bruker Avance 400 FT NMR spectrometer.  $^1\text{H}$  (500 MHz),  $^{13}\text{C}\{^1\text{H}\}$  (125 MHz), and  $^{29}\text{Si}\{^1\text{H}\}$  (100 MHz) NMR spectra of products were recorded on a Bruker Ascent 500FT NMR spectrometer. Sampling of air-sensitive materials was carried out using a VAC Nexus 100027-type glove box. Mass spectra were obtained on a JEOL JMS-600W mass spectrometer. UV-vis spectra and emission spectra were recorded on a JASCO V-660 and a Hitachi F-4500 spectrometers, respectively.

### 4.2 | Materials

All solvents treating air-sensitive compounds were dried prior to use. THF was dried over potassium mirror and then distilled prior to use by using a vacuum line. DMF was dried over  $\text{CaH}_2$  and filtered off, then distilled under reduced pressure. Thus, obtained DMF was stored in the presence of molecular sieves 4A. Toluene was dried over lithium aluminum hydride and then distilled prior to use. THF- $d_8$  and DMSO- $d_6$  were dried over molecular sieves 4A and degassed prior to use by using a vacuum line. Other solvents (dry ether, ethyl acetate, chloroform and chloroform- $d$ , and hexane) were used as received without further purification. 1,2-Dibromobenzene, 2-bromopropane, anhydrous LiCl, magnesium turnings, dichlorosilane,  $\text{LiAlH}_4$ , *tert*-butyllithium, and [2.2.2]cryptand were used as received. 2-bromophenylmagnesium bromide was prepared according to the reported method.<sup>[22]</sup>

### 4.2.1 | Improved synthesis of bis(2-bromophenyl)silane 2

In a three-necked flask equipped with a magnetic stir bar, 1,2-dibromobenzene (65.9 g, 279 mmol) was added to the solution of  $^i\text{PrMgBr}\cdot\text{LiCl}$  in THF (0.75 mol/L, 310 mL) at  $-25^\circ\text{C}$ , and thus, obtained solution was stirred for 2.5 hours. Then, THF solution (56 mL) of dichlorosilane (14.0 g, 139 mmol) was added to the reaction mixture at  $-80^\circ\text{C}$ , and the reaction mixture was stirred for 1 hour. The resulting solution was hydrolyzed with saturated aqueous  $\text{NH}_4\text{Cl}$  and then extracted with ether. The combined organic layer was washed with brine, dried over anhydrous  $\text{MgSO}_4$ , and evaporated to afford a crude product. The crude product was purified by Kugelrohr distillation ( $60^\circ\text{C}$ , 1.5 Pa), and the distillate was washed with methanol. Pure product was obtained as a colorless solid in 75% yield (71.6 g, 209 mmol). The spectroscopic data of the product were identical to those in the previous report.<sup>[12]</sup>

### 4.2.2 | 9-(2-Formylphenyl)-9,10-disilatriptycene (4)

In a triple-necked flask equipped with a magnetic stir bar and a reflux condenser, THF (20 mL) was added to the mixture of magnesium turnings (802 mg, 33.0 mmol) and **2** (4.80 g, 14.0 mmol) at room temperature and the reaction mixture was stirred for 10 hours with reflux. Then, DMF (12 mL, 156 mmol) was added dropwise to the reaction mixture at  $0^\circ\text{C}$  for 1 hour. The resulting solution was hydrolyzed with saturated aqueous  $\text{NH}_4\text{Cl}$  and was extracted with ether. The combined organic layer was washed with brine, dried over anhydrous  $\text{Na}_2\text{SO}_4$ , and evaporated to afford crude **4**. Pure **4** was obtained by silica-gel column chromatography (eluent:hexane/ $\text{CHCl}_3$  5:1) as a colorless solid in 18% yield (491 mg, 1.26 mmol).

**4**: a colorless solid; mp  $257\text{--}258^\circ\text{C}$ ;  $^1\text{H}$  NMR (chloroform- $d$ , 400 MHz, 297 K)  $\delta$  5.61 (s,  $^1J_{\text{Si-H}} = 220$  Hz, 1H, SiH), 7.18–7.25 (m, 6H), 7.64 (d,  $J = 6.8$  Hz, 3H), 7.86–7.89 (m, 4H), 7.94 (dt,  $J = 7.6, 1.6$  Hz, 1H), 8.35 (d,  $J = 7.6$  Hz, 1H), 8.75 (d,  $J = 7.2$  Hz, 1H), 10.15 (s, 1H, CHO);  $^{13}\text{C}\{^1\text{H}\}$  NMR (chloroform- $d$ , 100 MHz, 298 K)  $\delta$  127.7 (CH), 127.9 (CH), 129.3 (CH), 131.6 (CH and C, overlapping), 133.0 (CH), 133.3 (CH), 133.9 (CH), 137.7 (CH), 143.1 (C), 144.25 (C), 144.32 (C), 192.5 (CHO);  $^{29}\text{Si}\{^1\text{H}\}$  NMR (chloroform- $d$ , 79.5 MHz, 298 K)  $\delta$   $-39.0$  (SiAr),  $-36.6$  (SiH); IR (KBr,  $\text{cm}^{-1}$ ) 3039 ( $\nu_{\text{C-H}}$ ), 2191 ( $\nu_{\text{Si-H}}$ ), 1700 ( $\nu_{\text{C=O}}$ ), 1429; MS (EI, 70 eV) 390 (12,  $\text{M}^+$ ), 345 (4), 312 (2), 268 (8), 92 (100); Anal. Calcd for  $\text{C}_{25}\text{H}_{18}\text{OSi}_2$ : C, 76.88; H, 4.65. Found: C, 76.74, H, 4.73.

### 4.2.3 | 9-(2-Hydroxymethylphenyl)-9,10-disilatriptycene 5

In a Schlenk tube equipped with a magnetic stir bar, a suspension of **4** (1.08 g, 2.77 mmol) in ether (59 mL) was added to

a suspension of  $\text{LiAlH}_4$  (55 mg, 1.45 mmol) in ether (29 mL) at  $0^\circ\text{C}$ . After stirred for 40 minutes, the reaction mixture was hydrolyzed with saturated aqueous  $\text{NH}_4\text{Cl}$ . The resulting solution was extracted with ether. The combined organic layer was washed with brine, dried over anhydrous  $\text{Na}_2\text{SO}_4$ , and evaporated to afford crude **5**. Pure **5** was obtained by silica-gel column chromatography (eluent:hexane/AcOEt 3:1) as a colorless solid in 83% yield (901 mg, 2.30 mmol).

**5**: a colorless solid; mp  $213\text{--}214^\circ\text{C}$ ;  $^1\text{H}$  NMR (chloroform-*d*, 400 MHz, 300 K)  $\delta$  1.65 (t,  $J = 5.2$  Hz, 1H, OH), 4.73 (d,  $J = 5.2$  Hz, 2H,  $\text{CH}_2$ ), 5.59 (s,  $^1J_{\text{Si-H}} = 219$  Hz, 1H, Si-H), 7.19–7.25 (m, 6H), 7.61 (t,  $J = 7.6$  Hz, 1H), 7.68–7.73 (m, 3H), 7.76 (t,  $J = 6.8$  Hz, 1H), 7.83–7.87 (m, 3H), 7.92 (d,  $J = 7.6$  Hz, 1H), 8.55 (d,  $J = 6.8$  Hz, 1H);  $^{13}\text{C}\{^1\text{H}\}$  NMR (chloroform-*d*, 100 MHz, 300 K)  $\delta$  65.5 ( $\text{CH}_2$ ), 126.0 (C), 127.5 (CH), 127.7 (CH), 127.8 (CH), 129.2 (CH), 131.7 (CH), 133.0 (CH), 133.3 (CH), 136.7 (CH), 144.4 (C), 144.8 (C), 148.8 (C);  $^{29}\text{Si}\{^1\text{H}\}$  NMR (chloroform-*d*, 79.5 MHz, 299 K)  $\delta$   $-39.1$  (SiAr),  $-36.6$  (SiH); IR (KBr,  $\text{cm}^{-1}$ ) 3579 ( $\nu_{\text{O-H}}$ ), 3039 ( $\nu_{\text{C-H}}$ ), 2168 ( $\nu_{\text{Si-H}}$ ), 1422; MS (EI, 70 eV) 391 (31,  $M^+ - 1$ ), 314 (8), 269 (9), 92 (100); Anal. Calcd for  $\text{C}_{25}\text{H}_{20}\text{OSi}_2$ : C, 76.48; H, 5.13. Found: C, 76.52, H, 5.39.

#### 4.2.4 | $[\text{Li}(\text{thf})]^+6^-$

In a Schlenk tube equipped with a magnetic stir bar, a pentane solution of *tert*-butyllithium (1.39 mol/L, 0.37 mL) was added dropwise to a THF solution (1 mL) of **5** (200 mg, 510  $\mu\text{mol}$ ) at  $-78^\circ\text{C}$  and the resulting solution was stirred for 1 hour. After removal of the volatiles, the reaction mixture was washed with dry hexane, and then, the solvent was evaporated. The salt  $[\text{Li}(\text{thf})]^+6^-$  was obtained as a colorless solid in 80% yield (192 mg, 408  $\mu\text{mol}$ ). As compound  $[\text{Li}(\text{thf})]^+6^-$  gradually decomposed even in the solid state, elemental analysis was not conducted.

$[\text{Li}(\text{thf})]^+6^-$ : a colorless solid; mp  $195^\circ\text{C}$  (decomposed);  $^1\text{H}$  NMR (DMSO-*d*<sub>6</sub>, 400 MHz, 297 K)  $\delta$  1.73–1.80 (m, 4H), 3.55–3.64 (m, 4H), 4.91 (s, 2H,  $\text{CH}_2$ ), 5.14 (s, 1H, SiH), 6.41 (d,  $J = 7.0$  Hz, 1H), 6.72 (t,  $J = 7.0$  Hz, 1H), 6.80–6.87 (m, 6H), 7.00 (t,  $J = 7.0$  Hz, 1H), 7.08 (d,  $J = 7.0$  Hz, 1H), 7.38 (d,  $J = 6.4$  Hz, 3H), 7.45 (d,  $J = 6.4$  Hz, 3H);  $^{13}\text{C}\{^1\text{H}\}$  NMR (DMSO-*d*<sub>6</sub>, 100 MHz, 298 K)  $\delta$  25.2 ( $\text{CH}_2$ , THF), 63.7 ( $\text{CH}_2$ ), 67.0 ( $\text{CH}_2$ , THF), 120.2 (CH), 122.6 (CH), 123.9 (CH), 124.5 (CH), 125.4 (CH), 130.4 (CH), 134.9 (CH), 135.4 (CH), 144.8 (C), 149.5 (C), 153.4 (C), 166.1 (C);  $^{29}\text{Si}\{^1\text{H}\}$  NMR (DMSO-*d*<sub>6</sub>, 79.5 MHz, 297 K)  $\delta$   $-41.1$  (SiH),  $-104.4$  (Si).

#### 4.2.5 | $[\text{Li}(\text{thf})]^+7^-$

In a Schlenk tube equipped with a magnetic stir bar, a pentane solution of *tert*-butyllithium (1.39 mol/L, 0.21 mL) was added dropwise to a THF solution (0.2 mL) of **5** (51 mg, 130  $\mu\text{mol}$ ) at  $-78^\circ\text{C}$  and stirred for 1 hour. After removal

of the volatiles, the resulting mixture was washed with dry hexane, and then, the solvent was evaporated. The salt  $[\text{Li}(\text{thf})]^+7^-$  was obtained as a colorless solid in 82% yield (56 mg, 107  $\mu\text{mol}$ ). As compound  $[\text{Li}(\text{thf})]^+7^-$  gradually decomposed even in the solid state, elemental analysis was not conducted.

$[\text{Li}(\text{thf})]^+7^-$ : a colorless solid; mp  $264\text{--}265^\circ\text{C}$  (decomposed);  $^1\text{H}$  NMR (DMSO-*d*<sub>6</sub>, 400 MHz, 298 K)  $\delta$  1.72 (s, 9H), 1.73–1.1.80 (m, 4H), 3.58–3.63 (m, 4H), 4.88 (s, 2H,  $\text{CH}_2$ ), 6.30 (d,  $J = 7.2$  Hz, 1H), 6.66 (t,  $J = 7.2$  Hz, 1H), 6.77–6.79 (m, 6H), 6.95 (t,  $J = 7.2$  Hz, 1H), 7.04 (d,  $J = 7.2$  Hz, 1H), 7.38 (brs, 3H), 7.62–7.65 (m, 3H);  $^{13}\text{C}\{^1\text{H}\}$  NMR (DMSO-*d*<sub>6</sub>, 100 MHz, 300 K)  $\delta$  16.6 (C), 25.1 ( $\text{CH}_2$ , THF), 29.0 ( $\text{CH}_3$ ), 63.6 ( $\text{CH}_2$ ), 67.0 ( $\text{CH}_2$ , THF), 120.1 (CH), 121.9 (CH), 123.7 (CH), 124.3 (CH), 124.4 (CH), 130.0 (CH), 135.0 (CH), 135.6 (CH), 144.4 (C), 149.4 (C), 154.2 (C), 168.0 (C);  $^{29}\text{Si}\{^1\text{H}\}$  NMR (DMSO-*d*<sub>6</sub>, 79.5 MHz, 299 K)  $\delta$   $-37.5$  (Si-*t*-Bu),  $-105.2$  (Si).

#### 4.2.6 | $[\text{Li}(\text{crypt-222})]^+7^-$

In a Schlenk tube equipped with a magnetic stir bar, a toluene solution (1 mL) of crypt-222 (107 mg, 284  $\mu\text{mol}$ ) was added dropwise to a toluene solution (1 mL) of silicate  $[\text{Li}(\text{thf})]^+7^-$  (148 mg, 281  $\mu\text{mol}$ ) at room temperature and stirred for 1 day. Colorless solid was precipitated. The precipitate was washed with dry hexane, and then, the solvent was evaporated. Compound  $[\text{Li}(\text{crypt-222})]^+7^-$  was obtained as a colorless solid in 82% yield (192 mg, 230  $\mu\text{mol}$ ).

$[\text{Li}(\text{crypt-222})]^+7^-$ : a colorless solid; mp  $178\text{--}180^\circ\text{C}$  (decomposed);  $^1\text{H}$  NMR (DMSO-*d*<sub>6</sub>, 500 MHz, 300 K)  $\delta$  1.73 (s, 9H, *t*-Bu), 2.55 (s, 12H, crypt-222), 3.50 (s, 12H, crypt-222), 3.56 (s, 12H, crypt-222), 4.89 (s, 2H,  $\text{CH}_2$ ), 6.32 (d,  $J = 7.0$  Hz, 1H), 6.67 (t,  $J = 7.0$  Hz, 1H), 6.79 (brs, 6H), 6.96 (t,  $J = 7.0$  Hz, 1H), 7.05 (d,  $J = 7.0$  Hz, 1H), 7.39 (brs, 3H), 7.65 (brs, 3H);  $^{13}\text{C}\{^1\text{H}\}$  NMR (DMSO-*d*<sub>6</sub>, 126 MHz, 300 K)  $\delta$  16.7 (C), 29.0 ( $\text{CH}_3$ ), 55.7 ( $\text{CH}_2$ , crypt-222), 63.6 ( $\text{CH}_2$ ), 69.3 ( $\text{CH}_2$ , crypt-222), 70.1 ( $\text{CH}_2$ , crypt-222), 120.1 (CH), 122.0 (CH), 123.7 (CH), 124.3 (CH), 124.4 (CH), 130.0 (CH), 135.0 (CH), 135.7 (CH), 144.4 (C), 149.4 (C), 154.3 (C), 168.1 (C);  $^{29}\text{Si}\{^1\text{H}\}$  NMR (DMSO-*d*<sub>6</sub>, 99.4 MHz, 300 K)  $\delta$   $-37.5$  (Si-*t*-Bu),  $-105.2$  (Si); Anal. Calcd for  $\text{C}_{47}\text{H}_{63}\text{LiN}_2\text{O}_7\text{Si}_2$ : C, 67.92; H, 7.64. Found: C, 67.77, H, 7.57.

#### 4.2.7 | 9-*tert*-Butyl-10-(2-hydroxymethylphenyl)-9,10-disilatriptycene **8**

In a Schlenk tube equipped with a magnetic stir bar, a solution of silicate  $[\text{Li}(\text{thf})]^+7^-$  (204 mg, 387  $\mu\text{mol}$ ) in THF (2 mL) was reacted with saturated aqueous  $\text{NH}_4\text{Cl}$  (1 mL) at room temperature for 20 minutes. Then, the reaction mixture was extracted with ether, and the combined

organic layer was washed with brine, dried over anhydrous  $\text{Na}_2\text{SO}_4$ , and evaporated to afford crude **8**. Pure **8** was obtained by silica-gel column chromatography (eluent:hexane/AcOEt 3:1) as a colorless solid in 62% yield (108 mg, 240  $\mu\text{mol}$ ).

**8**: a colorless solid; mp 201–204°C (decomposed);  $^1\text{H}$  NMR (chloroform-*d*, 500 MHz, 299 K)  $\delta$  1.62 (t,  $J = 5.0$  Hz, 1H, OH), 1.84 (s, 9H, *t*-Bu), 4.68 (d,  $J = 5.0$  Hz, 2H,  $\text{CH}_2$ ), 7.16–7.25 (m, 6H), 7.61 (dt,  $J = 7.5, 1.0$  Hz, 1H), 7.72 (dd,  $J = 7.0, 0.5$  Hz, 3H), 7.75 (dt,  $J = 7.5, 1.0$  Hz, 1H), 7.92 (d,  $J = 7.5$  Hz, 1H), 8.02 (dd,  $J = 7.0, 0.5$  Hz, 3H), 8.56 (dd,  $J = 7.5, 1.0$  Hz, 1H);  $^{13}\text{C}\{^1\text{H}\}$  NMR (chloroform-*d*, 126 MHz, 300 K)  $\delta$  17.3 (C), 28.9 ( $\text{CH}_3$ ), 65.6 ( $\text{CH}_2$ ), 126.3 (C), 127.08 (CH), 127.10 (CH), 127.8 (CH), 129.3 (CH), 131.6 (CH), 133.2 (CH), 133.3 (CH), 136.7 (CH), 144.6 (C), 146.5 (C), 149.0 (C);  $^{29}\text{Si}\{^1\text{H}\}$  NMR (chloroform-*d*, 99.4 MHz, 299 K)  $\delta$  -32.3 (*Si*-Bu), -40.0 (Si); IR (KBr,  $\text{cm}^{-1}$ ) 3579 ( $\nu_{\text{O-H}}$ ), 3041 ( $\nu_{\text{C-H}}$ ), 1430; MS (EI, 70 eV) 447 (4,  $[\text{M} - \text{H}]^+$ ), 391 (100), 374 (3), 283 (2), 239 (11), 211 (9), 181 (18), 105 (13); Anal. Calcd for  $\text{C}_{29}\text{H}_{28}\text{OSi}_2$ : C, 77.63; H, 6.29. Found: C, 77.60, H, 6.32.

### 4.3 | X-ray analysis

Compounds **4**, **5**, and **8** were recrystallized by slow cooling of the toluene solution from 90°C to room temperature to grow single crystals suitable for XRD analysis. Single crystals of  $[\text{Li}(\text{crypt-222})]^+7^-$  were obtained by a slow diffusion method; toluene solution of crypt-222 was put on toluene solution of  $[\text{Li}(\text{thf})]^+7^-$  at room temperature. The single crystals coated by Apiezon<sup>®</sup> grease were mounted on a thin glass fiber and transferred to the cold nitrogen gas stream of the diffractometer. X-ray data were collected on a Bruker AXS APEX II CCD diffractometer with graphite monochromated Mo-K $\alpha$  radiation. An empirical absorption correction based on the multiple measurement of equivalent reflections was applied using the program SADABS.<sup>[23]</sup> Structures were solved by direct methods and refined by full-matrix least squares against  $F^2$  using all data (SHELXL-2014<sup>[24]</sup> and Yadokari-XG software<sup>[25]</sup>). The supplementary crystallographic data for this paper (CCDC-1864982 to 1864985) can be obtained free of charge from The Cambridge Crystallographic Data Centre via [www.ccdc.cam.ac.uk/data\\_cif](http://www.ccdc.cam.ac.uk/data_cif).

Crystal data for **4** (CCDC-1864982) (100 K): 0.20 mm  $\times$  0.20 mm  $\times$  0.05 mm;  $\text{C}_{25}\text{H}_{18}\text{OSi}_2$ ; Formula weight 390.57; monoclinic; space group  $P2_1/n$  (#14);  $a = 11.175(2)$  Å,  $b = 12.536(2)$  Å,  $c = 13.678(3)$  Å,  $\beta = 92.419(2)^\circ$ ,  $V = 1914.6(6)$  Å<sup>3</sup>,  $Z = 4$ ,  $D_{\text{calcd}} = 1.355$  Mg/m<sup>3</sup>, 9555 reflections measured, 3748 unique ( $R_{\text{int}} = 0.0488$ ), which were used in all calculations;  $R1 = 0.0489$  ( $I > 2\sigma(I)$ ),  $wR2 = 0.1349$  (all data),  $\text{GOF} = 1.030$ , max/min residual electron densities 0.713/−0.629 e Å<sup>−3</sup>.

Crystal data for **5** (CCDC-1864983) (100 K): 0.30 mm  $\times$  0.03 mm  $\times$  0.03 mm;  $\text{C}_{25}\text{H}_{20}\text{OSi}_2$ ; Formula weight 392.59; monoclinic; space group  $Cc$  (#9);  $a = 10.908(3)$  Å,  $b = 20.750(5)$  Å,  $c = 8.759(2)$  Å,  $\beta = 100.650(3)^\circ$ ,  $V = 1948.5(8)$  Å<sup>3</sup>,  $Z = 4$ ,  $D_{\text{calcd}} = 1.338$  Mg/m<sup>3</sup>, 2833 reflections measured, 2833 unique ( $R_{\text{int}} = 0.0311$ ), which were used in all calculations;  $R1 = 0.0391$  ( $I > 2\sigma(I)$ ),  $wR2 = 0.1141$  (all data),  $\text{GOF} = 1.059$ , max/min residual electron densities 0.460/−0.325 e Å<sup>−3</sup>.

Crystal data for  $[\text{Li}(\text{crypt-222})]^+7^-$  (CCDC-1864985) (100 K): 0.20 mm  $\times$  0.10 mm  $\times$  0.05 mm;  $\text{C}_{47}\text{H}_{63}\text{LiN}_2\text{O}_7\text{Si}_2$ ; Formula weight 831.11; triclinic; space group  $P-1$  (#2);  $a = 11.7509(13)$  Å,  $b = 12.5126(13)$  Å,  $c = 16.5442(18)$  Å,  $\alpha = 83.5840(10)^\circ$ ,  $\beta = 87.9320(10)^\circ$ ,  $\gamma = 65.7070(10)^\circ$ ,  $V = 2203.2(4)$  Å<sup>3</sup>,  $Z = 2$ ,  $D_{\text{calcd}} = 1.253$  Mg/m<sup>3</sup>, 11 656 reflections measured, 8847 unique ( $R_{\text{int}} = 0.0263$ ), which were used in all calculations;  $R1 = 0.0460$  ( $I > 2\sigma(I)$ ),  $wR2 = 0.1246$  (all data),  $\text{GOF} = 1.025$ , max/min residual electron densities 0.552/−0.439 e Å<sup>−3</sup>.

Crystal data for **8** (CCDC-1864984) (100 K): 0.40 mm  $\times$  0.05 mm  $\times$  0.04 mm;  $\text{C}_{29}\text{H}_{28}\text{OSi}_2$ ; Formula weight 448.69; monoclinic; space group  $P2_1/n$  (#14);  $a = 12.9056(10)$  Å,  $b = 11.4774(8)$  Å,  $c = 16.5672(12)$  Å,  $\beta = 107.7400(10)^\circ$ ,  $V = 2337.3(3)$  Å<sup>3</sup>,  $Z = 4$ ,  $D_{\text{calcd}} = 1.275$  Mg m<sup>−3</sup>, 11 931 reflections measured, 4574 unique ( $R_{\text{int}} = 0.0217$ ), which were used in all calculations;  $R1 = 0.0377$  ( $I > 2\sigma(I)$ ),  $wR2 = 0.0980$  (all data),  $\text{GOF} = 1.022$ , max/min residual electron densities 0.578/−0.257 e Å<sup>−3</sup>.

### 4.4 | Theoretical study

All theoretical calculations were performed using a Gaussian 09<sup>[26]</sup> and GRRM 14<sup>[27]</sup> programs. Geometrical optimization and frequency analysis were carried out at the B3PW91 + D3/6-31 + G(d) level of theory. Initially, the optimized structures of two rotamers of **6<sup>−</sup>** (**6a<sup>−</sup>** and **6b<sup>−</sup>**) are calculated; then, the transition state **6<sub>TS</sub><sup>−</sup>** that connects **6a<sup>−</sup>** and **6b<sup>−</sup>** was computed using 2PSHS method.<sup>[28]</sup> No imaginary frequencies were found in the equilibrium structures of **6a<sup>−</sup>**, **6b<sup>−</sup>**, and **6t<sup>−</sup>**, whereas one imaginary frequency was found in a transition state (**6<sub>TS</sub><sup>−</sup>**). Atomic coordinates of the optimized structures of the compounds with energy with zero-point correction are summarized in Tables S1–S4 in the Supporting Information. The reaction path from **6a<sup>−</sup>** to **6b<sup>−</sup>** via **6<sub>TS</sub><sup>−</sup>** was confirmed by IRC calculation.<sup>[29]</sup> An animated GIF file (IRC\_trace.gif) that represents the above IRC trace was prepared using ChemCraft.<sup>[30]</sup>

### ACKNOWLEDGMENTS

This work was supported by the Cooperative Research Program of “Network Joint Research Center for Materials

and Devices" (S.I.), JSPS KAKENHI [Nos. JP25708004 and JP25620020 (S.I.)].

## ORCID

Shintaro Ishida  <https://orcid.org/0000-0001-7832-912X>

Takeaki Iwamoto  <https://orcid.org/0000-0002-8556-5785>

## REFERENCES

- Reviews on silicates, see: a) R. R. Holmes, *Chem. Rev.* **1990**, *90*, 17; b) C. Chuit, R. J. P. Corriu, C. Reye, J. C. Young, *Chem. Rev.* **1993**, *93*, 1371; c) D. Kost, I. Kalikhman, in *The Chemistry of Organic Silicon Compounds*, Vol. 2 (Eds: Z. Rappoport, Y. Apeloig), Wiley, Chichester **1998**, Ch. 23; d) E. P. A. Couzijn, J. C. Slootweg, A. W. Ehlers, K. Lammertsma, *Z. Anorg. Allg. Chem.* **2009**, *635*, 1273; e) J. Wagler, U. Böhme, E. Kroke, in *Structure and Bonding 155, Functional Molecular Silicon Compounds I* (Ed: D. Scheschkewitz), Regular oxidation states. Springer International Publishing, Switzerland **2014**, pp. 29–105; f) G. Singh, G. Kaur, J. Singh, *Inorg. Chem. Commun.* **2018**, *88*, 11.
- a) K. Tamao, T. Kakui, M. Akita, T. Iwahara, R. Kanatani, J. Yoshida, M. Kumada, *Tetrahedron* **1983**, *39*, 983; b) K. Tamao, N. Ishida, T. Tanaka, M. Kumada, *Organometallics* **1983**, *2*, 1694; c) I. Fleming, R. Henning, H. Plaut, *J. Chem. Soc. Chem. Commun.* **1984**, 29.
- Hiyama coupling: a) Y. Hatanaka, T. Hiyama, *J. Org. Chem.* **1988**, *53*, 918; b) T. Hiyama, Y. Hatanaka, *Pure. Appl. Chem.* **1994**, *66*, 1471.
- Reviews on silyl migrations, see: a) A. G. Brook, A. R. Bassindale, in *Rearrangements in Ground and Excited States* (Ed: P. Mayo), Academic Press, London, UK **1980**, Vol. 2, Essay 9; b) E. W. Colvin, in *Silicon in Organic Synthesis*, Academic Press, Butterworths, FL, USA **1981**, Ch. 5; c) M. Kira, T. Iwamoto, in *The Chemistry of Organic Silicon Compounds* (Eds: Z. Rappoport, Y. Apeloig), Wiley, Chichester **2001**, Vol. 3, Ch. 16.
- Dehydrogenative C–H silylation: a) A. A. Toutov, W.-B. Liu, K. N. Betz, A. Fedorov, B. M. Stoltz, R. H. Grubbs, *Nature* **2015**, *518*, 80; b) W.-B. Liu, D. P. Schuman, Y.-F. Yang, A. A. Toutov, Y. Liang, H. F. T. Klare, N. Nesnas, M. Oestreich, D. G. Blackmond, S. C. Virgil, S. Banerjee, R. N. Zare, R. H. Grubbs, K. N. Houk, B. M. Stoltz, *J. Am. Chem. Soc.* **2017**, *139*, 6867.
- R. S. Berry, *J. Chem. Phys.* **1960**, *32*, 933.
- a) I. Ugi, D. Marquarding, H. Klusacek, P. Gillespie, F. Ramirez, *Acc. Chem. Res.* **1971**, *4*, 288; b) P. Lemmen, R. Baumgartner, I. Ugi, F. Ramirez, *Chem. Scr.* **1988**, *28*, 451.
- E. P. A. Couzijn, J. C. Slootweg, A. W. Ehlers, K. Lammertsma, *J. Am. Chem. Soc.* **2010**, *132*, 18127.
- Five-coordinate silicates with rigid bidentate ligands: a) R. Tacke, B. Pfrommer, M. Pülm, R. Bertermann, *Eur. J. Inorg. Chem.* **1999**, 807; E. P. A. Couzijn, M. Schakel, F. J. J. de Kanter, A. W. Ehlers, M. Lutz, A. L. Spek, K. Lammertsma, *Angew. Chem. Int. Ed.* **2004**, *43*, 3440; c) S. Dragota, R. Bertermann, C. Burschka, M. Penka, R. Tacke, *Organometallics* **2005**, *24*, 5560; d) E. P. A. Couzijn, D. W. F. van den Engel, J. C. Slootweg, F. J. J. de Kanter, A. W. Ehlers, M. Schakel, K. Lammertsma, *J. Am. Chem. Soc.* **2009**, *131*, 3741; e) L. J. P. van der Boon, L. van Gelderen, T. R. de Groot, M. Lutz, J. C. Slootweg, A. W. Ehlers, K. Lammertsma, *Inorg. Chem.* **2018**, *57*, 12697.
- Related constraint five-coordinate phosphorous compounds, see: a) P. Gillespie, P. Hoffman, H. Klusacek, D. Marquarding, S. Pfohl, F. Ramirez, E. A. Tsolis, I. Ugi, *Angew. Chem. Int. Ed. Engl.* **1971**, *10*, 687; b) F. Ramirez, I. Ugi, F. Lin, S. Pfohl, P. Hoffman, D. Marquarding, *Tetrahedron* **1974**, *30*, 371; c) F. Ramirez, Y. F. Chaw, J. F. Marecek, I. Ugi, *J. Am. Chem. Soc.* **1974**, *96*, 2429.
- S. Matsukawa, H. Yamamichi, Y. Yamamoto, K. Ando, *J. Am. Chem. Soc.* **2009**, *131*, 3418.
- T. Kuribara, S. Ishida, T. Kudo, S. Kyushin, *Organometallics* **2013**, *32*, 2092.
- Previously, compound **2** was prepared in 5 g scale; the reaction of 1-bromo-2-lithiobenzene with trichlorosilane to form bis(2-bromophenyl)chlorosilane and the following hydride reduction using  $\text{LiAlH}_4$  (50% isolated yield by two steps).<sup>[12]</sup> We developed a scalable and improved synthetic method of **2** using 2-bromophenylmagnesium bromide and dichlorosilane. For details, see experimental section.
- a) A. Bondi, *J. Phys. Chem.* **1964**, *68*, 441; b) W. S. Sheldrick, in *The Chemistry of Organic Silicon Compounds* (Eds: S. Patai, Z. Rappoport), Wiley, New York **1989**, Vol. 1, Chap. 3, pp. 227–303.
- The five-coordination characters, %TBPa and %TBPe, have been used as indicators of the structure about the central element in terms of the percentage trigonal bipyramidal geometry on the basis of the Ra–Si–Re (Ra: substituent at the apical position, Re: substituent at the equatorial position) bond angles and Re–Si–Re bond angles, respectively. For details, see ref 16.
- a) K. Tamao, T. Hayashi, Y. Ito, M. Shiro, *Organometallics* **1992**, *11*, 2099; b) N. Kano, A. Kikuchi, T. Kawashima, *Chem. Commun.* **2001**, 2096.
- Muetterties' rule predicts that more electronegative elements occupy the apical positions in five-valent compounds. For details, see: a) E. L. Muetterties, W. Mahler, R. Schmutzler, *Inorg. Chem.* **1963**, *2*, 613; b) E. L. Muetterties, W. Mahler, K. J. Packer, R. Schmutzler, *Inorg. Chem.* **1964**, *3*, 1298.
- a) S. Yamaguchi, S. Akiyama, K. Tamao, *J. Am. Chem. Soc.* **2000**, *122*, 6793; b) H. Lenormand, J.-P. Goddard, L. Fensterbank, *Org. Lett.* **2013**, *15*, 748.
- Generally, benzaldehydes are weak or non-fluorescent, see: a) J. W. Bridges, R. T. Williams, *Nature* **1962**, *196*, 59; b) R. T. Williams, J. W. Bridges, *J. Clin. Path.* **1964**, *17*, 371; c) K. Fletcher, U. H. F. Bunz, A. Dreuw, *ChemPhysChem* **2016**, *17*, 2650.
- a) D. A. Dixon, W. R. Hertler, D. B. Chase, W. B. Farnham, F. Davidson, *Inorg. Chem.* **1988**, *27*, 4012; b) A. H. J. F. de Keijzer, F. J. J. de Kanter, M. Schakel, R. F. Schmitz, G. W. Klumpp, *Angew. Chem. Int. Ed.* **1996**, *35*, 1127; c) T. Kawashima, K. Naganuma, R. Okazaki, *Organometallics* **1998**, *17*, 367.
- The topological parameter (TP) is defined by the following equation:  $\text{TP} = (\theta_{\text{ap}} - \theta_{\text{eq}})/60$ , where  $\theta_{\text{ap}}$  is the largest bond angle around the five-coordinate silicon atoms (usually Ra–Si–Ra) and  $\theta_{\text{eq}}$  is the largest angle between two equatorial ligands (Re–Si–Re) (usually second largest bond angle). If  $\text{TP} = 1$ , the structure is a pure trigonal bipyramidal structure, while if  $\text{TP} = 0$ , the structure is pure square pyramidal structure. For details, see ref 8.
- a) A. Krasovskiy, P. Knochel, *Angew. Chem. Int. Ed.* **2004**, *43*, 3333; b) A. Krasovskiy, P. Knochel, *Synthesis* **2006**, *5*, 890.

- [23] G. M. Sheldrick, SADABS, Empirical Absorption Correction Program, University of Göttingen, Göttingen, Germany **1996**.
- [24] G. M. Sheldrick, SHELXL-2014, Program for the Refinement of Crystal Structures, University of Göttingen, Göttingen, Germany **2014**.
- [25] Yadokari-XG 2009, Release of Software for Crystal Structure Analyses, C. Kabuto, S. Akine, T. Nemoto, E. Kwon, *J. Cryst. Soc. Jpn.* **2009**, *51*, 218.
- [26] M. J. Frisch, G. W. Trucks, H. B. Schlegel, G. E. Scuseria, M. A. Robb, J. R. Cheeseman, G. Scalmani, V. Barone, B. Mennucci, G. A. Petersson, H. Nakatsuji, M. Caricato, X. Li, H. P. Hratchian, A. F. Izmaylov, J. Bloino, G. Zheng, J. L. Sonnenberg, M. Hada, M. Ehara, K. Toyota, R. Fukuda, J. Hasegawa, M. Ishida, T. Nakajima, Y. Honda, O. Kitao, H. Nakai, T. Vreven, J. A. Montgomery Jr., J. E. Peralta, F. Ogliaro, M. Bearpark, J. J. Heyd, E. Brothers, K. N. Kudin, V. N. Staroverov, R. Kobayashi, J. Normand, K. Raghavachari, A. Rendell, J. C. Burant, S. S. Iyengar, J. Tomasi, M. Cossi, N. Rega, J. M. Millam, M. Klene, J. E. Knox, J. B. Cross, V. Bakken, C. Adamo, J. Jaramillo, R. Gomperts, R. E. Stratmann, O. Yazyev, A. J. Austin, R. Cammi, C. Pomelli, J. W. Ochterski, R. L. Martin, K. Morokuma, V. G. Zakrzewski, G. A. Voth, P. Salvador, J. J. Dannenberg, S. Dapprich, A. D. Daniels, Ö. Farkas, J. B. Foresman, J. V. Ortiz, J. Cioslowski, D. J. Fox, Gaussian 09, Revision D.01, Gaussian, Inc., Wallingford CT **2009**.
- [27] GRRM14, S. Maeda, Y. Harabuchi, Y. Osada, T. Taketsugu, K. Morokuma, K. Ohno see <http://grrm.chem.tohoku.ac.jp/GRRM/>;
- a) S. Maeda, K. Ohno, K. Morokuma, *Phys. Chem. Chem. Phys.* **2013**, *15*, 3683; b) S. Maeda, K. Ohno, K. Morokuma, *J. Chem. Theory Comput.* **2009**, *5*, 2734; c) S. Maeda, E. Abe, M. Hatanaka, T. Taketsugu, K. Morokuma, *J. Chem. Theory Comput.* **2012**, *8*, 5058.
- [28] For 2PSHS method, see: S. Maeda, K. Ohno, *Chem. Phys. Lett.* **2005**, *404*, 95.
- [29] For IRC calculation, see: a) K. Ishida, K. Morokuma, A. Komornicki, *J. Chem. Phys.* **1977**, *66*, 2153; b) K. Fukui, *Acc. Chem. Res.* **1981**, *14*, 363; c) M. Page, J. W. McIver Jr., *J. Chem. Phys.* **1988**, *88*, 922; d) C. Gonzalez, H. B. Schlegel, *J. Chem. Phys.* **1989**, *90*, 2154.
- [30] <http://www.chemcraftprog.com>.

## SUPPORTING INFORMATION

Additional supporting information may be found online in the Supporting Information section at the end of the article.

**How to cite this article:** Ishida S, Takiguchi M, Iwamoto T. Alkoxy(tetraaryl)silicates bearing 9,10-disilatriptycene skeleton. *Heteroatom Chem.* 2018;e21481. <https://doi.org/10.1002/hc.21481>